HHS Public Access

Author manuscript

Mol Psychiatry. Author manuscript; available in PMC 2021 October 13.

Published in final edited form as:

Mol Psychiatry. 2021 July ; 26(7): 3178–3191. doi:10.1038/s41380-020-00905-1.

Role of endocannabinoid signaling in a septohabenular pathway in the regulation of anxiety- and depressive-like behavior

Casey R. Vickstrom, PhD[1,2,*], **Xiaojie Liu, PhD**[1,2], **Shuai Liu**[1], **Meng-Ming Hu**[1], **Lianwei Mu**[1], **Ying Hu**[1], **Hao Yu**[1], **Santidra L. Love**[1], **Cecilia J. Hillard, PhD**[1], **Qing-song Liu, PhD**[1,*]

[1]Department of Pharmacology and Toxicology, Medical College of Wisconsin, Milwaukee, WI 53226

[2]These authors contributed equally to this work

Abstract

Enhancing endocannabinoid signaling produces anxiolytic- and antidepressant-like effects, but the neural circuits involved remain poorly understood. The medial habenula (MHb) is a phylogenetically-conserved epithalamic structure that is a powerful modulator of anxiety- and depressive-like behavior. Here, we show that a robust endocannabinoid signaling system modulates synaptic transmission between the MHb and its sole identified GABA input, the medial septum and nucleus of the diagonal band (MSDB). With RNAscope *in situ* hybridization, we demonstrate that key enzymes that synthesize or degrade the endocannabinoids 2-arachidonylglycerol (2-AG) or anandamide are expressed in the MHb and MSDB, and that cannabinoid receptor 1 (CB1) is expressed in the MSDB. Electrophysiological recordings in MHb neurons revealed that endogenously-released 2-AG retrogradely depresses GABA input from the MSDB. This endocannabinoid-mediated depolarization-induced suppression of inhibition (DSI) was limited by monoacylglycerol lipase (MAGL) but not by fatty acid amide hydrolase. Anatomic and optogenetic circuit mapping indicated that MSDB GABA neurons monosynaptically project to cholinergic neurons of the ventral MHb. To test the behavioral significance of this MSDB-MHb endocannabinoid signaling, we induced MSDB-specific knockout of CB1 or MAGL via injection of virally-delivered Cre recombinase into the MSDB of *Cnr1*$^{loxP/loxP}$ or *Mgll*$^{loxP/loxP}$ mice. Relative to control mice, MSDB-specific knockout of CB1 or MAGL bidirectionally modulated 2-AG signaling in the ventral MHb and led to opposing effects on anxiety- and depressive-like behavior. Thus, depression of synaptic GABA release in the MSDB-ventral MHb pathway may represent a potential mechanism whereby endocannabinoids exert anxiolytic and antidepressant-like effects.

[*]corresponding authors: Casey R. Vickstrom, Qing-song Liu, **Casey R Vickstrom:** 8701 Watertown Plank Rd. BSB617 Dept. of Pharmacology and Toxicology, Milwaukee, WI 53226, Phone: 414-955-4682, cvickstrom@mcw.edu, **Qing-song Liu:** 8701 Watertown Plank Rd. BSB617 Dept. of Pharmacology and Toxicology, Milwaukee, WI 53226, Phone: 414-955-8877, qsliu@mcw.edu.

Conflict of interest

The authors declare no conflicts of interest.

Introduction

Cross-sectional studies report that the majority of medical cannabis users use cannabis or other cannabinoids for anxiety and/or depression, and that cannabis improves self-reported symptoms of these disorders[1, 2]. In rodents, pharmacological inhibition of monoacylglycerol lipase (MAGL), the primary degradative enzyme for the endocannabinoid (eCB) 2-arachidonoylglycerol (2-AG)[3], had anxiolytic and antidepressant-like behavioral effects in mouse models of chronic[4, 5] and acute[6, 7] stress. Conversely, mice deficient in diacylglycerol lipase α (DAGLα), the major biosynthetic enzyme for 2-AG, displayed elevated anxiety-like behavior[8, 9]. Likewise, inhibition of fatty acid amide hydrolase (FAAH), the primary degradative enzyme for the eCB anandamide[10], had anxiolytic effects[6, 7]. Recent studies have begun to untangle the distinct neural circuits which mediate the anxiolytic and antidepressant-like effects of eCBs[11, 12], though there remains an incomplete understanding of the neural circuit basis of their action.

Emerging evidence has implicated the medial habenula (MHb) in the regulation of anxiety and depressive behavior. The MHb is an epithalamic structure that regulates anxiety- and depressive-like behavior in rodents[13–17] and its volume is decreased in humans with depression[18]. The MHb expresses mRNA and protein for DAGLα[19], suggesting that 2-AG may be released by MHb neurons and regulate anxiety- and depressive-like behavior by retrograde modulation of synaptic strength[20, 21].

The medial septum and nucleus of the diagonal band (MSDB) provides the sole identified GABAergic input to the MHb, as identified by retrograde tracing[22]. The MSDB has been implicated as a neural substrate of anxiety and mood-related behavior[23, 24], though the downstream circuits involved remain poorly understood. We hypothesized that 2-AG synthesized in the MHb produces anxiolytic and antidepressant-like behavioral effects via suppression of MSDB GABA input to the MHb. To test this hypothesis, we first used RNAscope fluorescent *in situ* hybridization (FISH)[25] to quantify the expression levels of components of the eCB system in the MSDB and MHb. Using slice electrophysiology, we show that 2-AG released from MHb neurons retrogradely suppresses synaptic GABA input. We further combined whole-cell electrophysiology with optogenetics and demonstrated that 2-AG acts at a selectively GABAergic input from the MSDB to cholinergic neurons of the ventral MHb. Lastly, viral-genetic knockout of CB1 or MAGL in the MSDB bidirectionally modulated 2-AG signaling in the MHb and led to opposing effects on anxiety- and depressive-like behavior, suggesting that eCB signaling in the MSDB-MHb pathway may exert anxiolytic- and antidepressant-like behavioral effects.

Results

The MHb expresses components of the eCB system

RNAscope FISH allows detection of single mRNA transcripts with high specificity and sensitivity[25]. We utilized RNAscope to quantify the expression of components of the eCB system in defined MHb neuron populations. The MHb is anatomically organized into dorsal and ventral subnuclei that express tachykinin 1 (Tac1) and choline acetyltransferase (ChAT), respectively[15]. DAGLα is the major enzyme for 2-AG synthesis[8, 9], whereas

N-acyl phosphatidylethanolamine-specific phospholipase D (NAPE-PLD) and fatty acid amide hydrolase (FAAH) synthesize and degrade the eCB anandamide, respectively[10, 26]. We observed mRNA expression of DAGLα, NAPE-PLD, and FAAH in the MHb (Fig. 1a–c). DAGLα, NAPE-PLD, and FAAH were expressed in both Tac1+ and ChAT+ cells. ChAT+ neurons expressed a significantly higher mRNA puncta density of these eCB system components than Tac1+ neurons (Fig. 1d). DAGLα puncta density was significantly higher than that of both NAPE-PLD and FAAH, and FAAH had a significantly higher puncta density than NAPE-PLD. These results suggest that the MHb may be an important locus for eCB signaling and that 2-AG signaling predominates over anandamide signaling in the MHb.

The eCB 2-AG suppresses GABAergic input to MHb neurons

Depolarization-induced suppression of excitation (DSE) or inhibition (DSI) is a form of retrograde depression mediated by Ca^{2+} influx-triggered, “on demand” synthesis and release of 2-AG[20, 21]. We made whole-cell recordings from putative cholinergic neurons in the ventral MHb in slices prepared from adult C57BL/6J mice, as well as cholinergic tdTomato+ neurons in ChAT-tdTomato reporter mice, which were generated by crossing ChAT-Cre mice with Ai9 mice[27]. GABA-mediated inhibitory postsynaptic currents (IPSCs) were evoked by electrical stimulation in the presence of the AMPA receptor antagonist CNQX (20 μM). Although $GABA_A$ receptor activation can be excitatory in MHb neurons[28, 29], we call these currents IPSCs to maintain convention. A brief depolarization (from −70 to 0 mV, 5 s) of ventral MHb neurons led to a transient suppression of IPSC amplitude (Fig. 1e). There was no significant difference in DSI amplitude in ventral MHb neurons from C57BL/6J mice relative to tdTomato+ neurons from ChAT-tdTomato mice ($t_{19} = 1.323$, $p = 0.202$), so these data were pooled. DSI was blocked by pretreatment of slices with the CB1 receptor antagonist AM251 (2 μM) or the DAGL inhibitor DO34 (1 μM) (Fig. 1e). The MAGL inhibitor JZL184 (1 μM) significantly prolonged DSI, as determined by the average time constant of its exponential decay, without significantly affecting DSI amplitude, whereas the FAAH inhibitor URB597 (1 μM) did not significantly affect DSI duration or amplitude (Supplementary Fig. 1). DSI amplitude was not significantly different between tdTomato+ neurons in the ventral MHb and putative Tac1+/tdTomato-negative neurons in the dorsal MHb in slices from ChAT-tdTomato reporter mice (Supplementary Fig. 2). Additionally, bath application of the CB1/CB2 receptor agonist WIN55212–2 (2 μM) decreased evoked IPSC amplitude (Fig. 1f) and increased the paired-pulse ratio (PPR) (Fig. 1g), suggesting a presynaptic mechanism whereby CB1 activation depresses GABA release. Thus, 2-AG released from MHb neurons induces short-term depression of synaptic GABA input by retrograde activation of CB1, and the duration of this depression is limited by MAGL but not FAAH activity.

We next tested whether cannabinoid-induced suppression of synaptic GABA input affects MHb neuron activity. As MHb action potential (AP) firing in *in vitro* slice conditions is not affected by the AMPA receptor antagonist CNQX and the $GABA_A$ receptor blocker picrotoxin[29, 30], we tested the effect of WIN55212–2 on electrical stimulation-induced, $GABA_A$ receptor-mediated excitation of AP firing. Unlike most regions in the adult brain, $GABA_A$ receptor activation can be excitatory in the MHb due to uniquely low expression of

the K^+/Cl^- co-transporter KCC2[28, 29]. We first determined the effects of $GABA_A$ receptor activation in MHb neurons. Cell-attached recordings were made so that intracellular [Cl^-] was not altered. The internal solution contained 0 or 10 μM of the fluorescent dye Alexa 594, as unwanted "spontaneous" mini-breaks into whole-cell mode can be detected by dye diffusion into the recorded cell. Pressure ejection of the $GABA_A$ agonist muscimol (2 μM) via a puff pipette (1–2 μm tip opening, 5 psi, 1 s) increased the frequency of AP firing in MHb neurons (Supplementary Fig. 3a). Additionally, in the presence of CNQX (20 μM), the NMDA receptor antagonist AP5 (50 μM), and the $GABA_B$ receptor antagonist CGP55845 (1 μM), burst (50 Hz, 5 stimuli) electrical stimulation increased the frequency of AP firing (Supplementary Fig. 3c). Muscimol and electrical stimulation-induced increases in AP firing were blocked by the $GABA_A$ receptor blocker picrotoxin (100 μM) (Supplementary Fig. 3b,d). In the presence of WIN55212–2 (2 μM), the effect of electrical stimulation to increase AP firing was significantly reduced (Supplementary Fig. 3e,f). Thus, CB1 activation reduced the excitatory effect of synaptic $GABA_A$ receptor activation on MHb neuron AP firing.

MSDB GABA neurons innervate the ventral MHb

What is the source of GABA input to MHb neurons? The MHb itself does not contain GABA neurons; rather, microinjection of the anatomical tracer biotinylated dextran amine (BDA) into the MHb in Gad1-GFP reporter mice identified the MSDB as the sole GABAergic input to the MHb[22]. However, BDA is a bidirectional tracer and can be taken up by damaged fibers-of-passage that do not form functional synapses in the target region[31]. Further, it does not reveal the cell-type-specific connectivity between structures. To overcome these limitations, we injected the adeno-associated virus (AAV) vector AAV1-phSyn1(S)-Flex-tdTomato-T2A-SypEGFP-WPRE into the MSDB of GAD2-Cre mice to selectively label GABA neurons (Fig. 2a). With this vector, the somata and axons of the transduced neurons express tdTomato, and putative synaptic contacts express synaptophysin-EGFP (SypEGFP). Synaptophysin is a major synaptic vesicle protein located in virtually all synapses[32]. Thus, this approach can distinguish direct synaptic connections from fibers-of-passage. After 4–5 weeks, expression of tdTomato was observed within the MSDB, indicating precise targeting (Fig. 2b). Expression of tdTomato and SypEGFP was abundant in the ventral MHb bilaterally (Fig. 2c). In the MHb, SypEGFP was expressed in close approximation to both the inhibitory postsynaptic marker gephyrin, which anchors and clusters postsynaptic $GABA_A$ receptors[33] (Supplementary Fig. 4a), and the dendritic and somatic protein microtubule-associated protein 2 (MAP2)[34] (Supplementary Fig. 4b). Thus, MSDB GABA neurons send axonal projections to the ventral MHb and form putative synaptic contacts with MHb neurons.

In addition to GABAergic neurons, the MSDB also contains glutamatergic and cholinergic neurons[35]. We determined whether the MSDB selectively sends a GABAergic input to the MHb and determined whether MSDB GABA neurons form functional synapses on MHb neurons. We injected AAV_{DJ}-ChR2(H134R)-GFP into the MSDB of ChAT-tdTomato reporter mice (Fig. 2d,e). After 2–3 weeks, ChR2(H134R)-GFP-expressing axon terminals were observed in the ventral MHb clustered around tdTomato+ MHb neurons (Fig. 2f). We prepared *ex vivo* brain slices and made whole-cell recordings from tdTomato+ neurons in the ventral MHb. Blue laser stimulation (473 nm, 3 ms) induced fast-onset IPSCs

that were blocked by picrotoxin (100 μM) and that were unaffected by CNQX (20 μM; Fig. 2g). Light-evoked IPSCs had an average reversal potential (E_{rev}) of −27.8 ± 1.2 mV, corrected for a calculated liquid junction potential of −7.7 mV (Fig. 2h). This is consistent with the calculated E_{rev} of Cl^-, based on Cl^- concentrations in the ACSF (128 mM) and pipet (50.2 mM) solutions (E_{Cl-} = −24.5 mV at 31°C). The average E_{rev} was not affected by CNQX (vehicle: −27.8 ± 1.2 mV, n = 15 neurons/N = 4 mice; CNQX: −25.3 ± 0.80 mV, n = 9 neurons/N = 3 mice; $t_{22} = -2.52$, $p = 0.138$). Lastly, in 4 of 4 independent experiments from the Allen Brain Atlas Mouse Brain Connectivity database (connectivity.brain-map.org), a projection from ChAT-expressing MSDB neurons to the MHb was not observed Supplementary (Fig. 5). Thus, the MSDB sends an exclusively GABAergic projection to neurons of the ventral MHb.

CB1 and MAGL mRNA are expressed in MSDB GABA neurons

As DSI was observed in the MHb, and as the MSDB is reported to be the only GABAergic input to the MHb[22], we determined whether MSDB GABA neurons express CB1 mRNA. We performed RNAscope for CB1 mRNA along with either the GABAergic neuron marker glutamate decarboxylase 1 (Gad1), the glutamatergic neuron marker vesicular glutamate transporter 2 (VGluT2), or the cholinergic neuron marker ChAT. CB1 mRNA was abundantly expressed in the MSDB, but not in neighboring regions (Fig. 3a). Greater than 90% of CB1-expressing MSDB neurons co-expressed mRNA for Gad1 (Fig. 3b; 1107 Gad1+/CB1+ of 1221 CB1+ cells, 90.7%). Nearly all MSDB Gad1-expressing neurons co-expressed CB1 (Fig. 3B; 1107 Gad1+/CB1+ of 1150 Gad1+ cells, 96.3%). A minority of CB1-expressing MSDB neurons co-expressed VGluT2 (Fig. 3B,S6; 432 VGluT2+/CB1+ of 3157 CB1+ cells; 13.7%) or ChAT (Fig. 3b, Supplementary Fig. 7; 185 ChAT+/CB1+ of 1752 CB1+ cells, 10.6%). CB1 mRNA was less abundant in MSDB VGluT2+ neurons relative to Gad1+ or ChAT+ neurons (Fig. 3a, Supplementary Figs. 6 & 7). MAGL is predominantly expressed in neuron presynaptic terminals[36]. MAGL mRNA was expressed in the MSDB, including in CB1+/Gad1+ neurons (Supplementary Fig. 8). Thus, CB1 and MAGL are expressed in MSDB GABA neurons, with CB1 predominantly expressed in MSDB GABA neurons. Together with DAGLα, NAPE-PLD, and FAAH, these studies indicate that a robust eCB signaling system is expressed in the MSDB and MHb.

2-AG specifically suppresses GABA input from the MSDB

We determined whether 2-AG released from MHb neurons acts at MSDB axon terminals in the ventral MHb. We injected AAV_{DJ}-DIO-ChR2(H134R)-GFP into the MSDB of GAD2-Cre mice, which resulted in ChR2-GFP expression in the ventral MHb 2–3 weeks after injection. We made whole-cell recordings in ventral MHb neurons in brain slices. GABA release from MSDB axon terminals was evoked by local blue light illumination (473 nm, 3 ms) from an optical fiber lowered to the recorded cell. Depolarization (from −70 to 0 mV, 5 sec) of MHb neurons led to robust DSI, which was blocked by pretreatment with AM251 (Fig. 4a). This indicates that 2-AG from ventral MHb neurons acts at CB1-expressing MSDB axon terminals to retrogradely depress GABA release.

Additionally, we injected AAV1.hSyn.HI.eGFP-Cre.WPRE.SV40 (AAV1-hSyn-Cre-eGFP) into the MSDB of *Cnr1*$^{loxP/loxP}$ or *Mgll*$^{loxP/loxP}$ mice to knock out (KO) CB1 or MAGL

from MSDB neurons. These mice are referred to as MSDB-CB1-KO and MSDB-MAGL-KO, respectively. C57BL/6J mice injected with AAV1-hSyn-Cre-eGFP in the MSDB (MSDB-WT mice) were the control for both knockouts. MHb slices were prepared from these mice 3–4 weeks following the AAV injection. Strikingly, DSI was absent in MHb neurons from MSDB-CB1-KO mice, whereas DSI duration was significantly prolonged in MHb neurons from MSDB-MAGL-KO mice relative to MSDB-WT mice (Fig. 4b). Immunostaining for Nissl in the MSDB after AAV1-hSyn-Cre-eGFP injection indicated that 88.9 ± 1.5% (n = 5 mice) of Nissl+ MSDB cells also expressed eGFP. The absence of DSI in MSDB-CB1-KO mice indicates that the MSDB likely provides the only CB1-expressing GABA input to the ventral MHb. Further, MSDB-specific CB1 or MAGL KO bidirectionally modulates 2-AG signaling at MSDB-MHb synapses.

Anxiety- and depressive-like behavior in MSDB-specific CB1 and MAGL knockouts

The MSDB[23, 24, 37], MHb[13, 15], and cannabinoids[38] are each independently linked to the regulation of anxiety and depressive-like behavior. We hypothesized that 2-AG signaling in the MSDB-MHb pathway is a neurobiological locus where these mechanisms converge. In a separate cohort of C57BL/6J, *Cnr1*$^{loxP/loxP}$, and *Mgll*$^{loxP/loxP}$ mice, AAV1-hSyn-Cre-eGFP was injected into the MSDB to induce loss- or gain-of-function in 2-AG/CB1 signaling in the ventral MHb. Beginning ~3–4 weeks after virus injection, anxiety- and depressive-like behaviors were assessed in these mice (Fig. 5a). Body weight was not significantly affected by MSDB-specific KO (Supplementary Fig. 9a).

Mice tend to avoid open spaces, and this avoidance behavior is responsive to anxiolytics[39–41]. In the open field test (OFT), total distance traveled was not significantly affected by MSDB-specific KO, but MSDB-CB1-KO mice spent less time in the center of a novel open field and made fewer entries into the center relative to MSDB-WT and MSDB-MAGL-KO mice. MSDB-CB1-KO mice also had a smaller percentage of distance traveled in the center area relative to MSDB-MAGL-KO mice (Fig. 5b). In the light-dark box test, MSDB-CB1-KO mice spent less time in the light box relative to MSDB-MAGL-KO mice (Supplementary Fig. 9b), but there was no significant effect of MSDB-specific KO on light-dark box transitions (Supplementary Fig. 9b) or elevated plus maze behavior (Supplementary Fig. 9c). Increased marble burying behavior reflects neophobic anxiety and is responsive to anxiolytics[42]. MSDB-CB1-KO mice buried significantly more marbles than MSDB-WT and MSDB-MAGL-KO mice in the marble burying test (MBT) (Fig. 5c), indicating increased neophobic anxiety in MSDB-CB1-KO mice. Thus, MSDB-CB1-KO mice had increased avoidance and neophobic anxiety behavior, whereas MSDB-MAGL-KO mice did not have significantly altered anxiety-like behavior relative to MSDB-WT mice.

Latency to feed in a novel open field in the novelty-suppressed feeding (NSF) test is sensitive to anxiolytics or chronic antidepressant treatment[43, 44]. MSDB-CB1-KO mice had a dramatic increase in the latency to feed in a novel open field relative to MSDB-WT and MSDB-MAGL-KO mice, without a significant change in latency to feed in the home cage, indicating increased anxiety/depressive-like behavior (Fig. 5d). Decreased sucrose preference in rodents is interpreted as a manifestation of anhedonia[45], which is a core feature of major depressive disorder[46]. Interestingly, MSDB-MAGL-KO mice had increased

sucrose preference relative to MSDB-WT and MSDB-CB1-KO mice (Fig. 5e), suggesting an antidepressant-like behavioral effect. Immobility in the forced swim test (FST) is a measure of behavioral despair and reflects a depressive phenotype[47]. MSDB-CB1-KO mice had greater immobility time relative to MSDB-MAGL-KO mice in the FST (Supplementary Fig. 9d). These phenotypes cannot be attributed to inherent behavioral differences between C57BL/6J, *Cnr1*$^{loxP/loxP}$, and *Mgll*$^{loxP/loxP}$ mice, as there were no significant differences between these mice in any of the aforementioned tests when not injected with AAV1-hSyn-Cre-eGFP (Supplementary Fig. 10). Together, these results indicate that MSDB-specific CB1 or MAGL KO led to opposing effects on anxiety- and/or depressive-like behavior in multiple behavioral tests.

Discussion

We have shown that the MSDB and MHb express a robust eCB system, and that activation of the CB1 receptor by endogenously-released 2-AG or an exogenous CB1 agonist led to depression of MSDB GABA input to cholinergic ventral MHb neurons. Loss- or gain-of-function of 2-AG/CB1 signaling in the MHb after MSDB-specific CB1 or MAGL KO led to elevated anxiety-like (MSDB-CB1-KO) and antidepressant-like (MSDB-MAGL-KO) behavioral effects in multiple behavioral tests. Collectively, these data suggest that this GABAergic MSDB-MHb pathway may be a critical locus where cannabinoids act to modulate anxiety- and depressive-like behaviors.

Traditional anatomical tracing studies suggested the presence of a projection from the MSDB to the MHb[22]. We found that expression of AAV1-Flex-tdTomato-T2A-SypEGFP in MSDB GABA neurons resulted in expression of both tdTomato and SypEGFP in the ventral MHb, suggesting that MSDB GABA neurons make direct synaptic contacts onto ventral MHb neurons. In support of this idea, SypEGFP was expressed in close approximation to MAP2 and gephyrin in the MHb. Further, optogenetic activation of MSDB axon terminals in the ventral MHb evoked $GABA_A$ receptor-mediated IPSCs in cholinergic MHb neurons. These rapid, light-evoked IPSCs were not affected by CNQX, indicating a direct, monosynaptic innervation of MHb neurons by MSDB GABA neurons, and that MSDB glutamate neurons do not innervate MHb neurons. A projection from cholinergic MSDB neurons to the MHb was not observed in 4 of 4 independent experiments from the Allen Brain Atlas Mouse Brain Connectivity database. Consistent with this, expression of ChR2-EYFP in MS cholinergic neurons did not lead to EYFP expression in the MHb[48]. Thus, the MSDB sends a selective GABAergic projection to cholinergic neurons in the ventral MHb. We showed that electrically-evoked IPSCs and DSI were observed in ChAT-negative neurons in the dorsal MHb. Consistent with this, spontaneous and evoked GABA IPSCs were previously observed in the dorsal MHb in mice[49]. However, GABAergic input to these putative Tac1 neurons remains to be identified.

We found that the MSDB and MHb express a robust eCB system. DAGLα, NAPE-PLD, and FAAH mRNA were expressed in the MHb, particularly in cholinergic ventral MHb neurons, indicating that MHb neurons are likely capable of 2-AG and anandamide synthesis. DAGLα expression was more abundant than that of NAPE-PLD or FAAH, suggesting that 2-AG signaling predominates over anandamide signaling. However, anandamide synthesis

can also occur via biochemical pathways that were not assessed in this study[50]. CB1 mRNA was abundantly expressed in MSDB GABA neurons, and MAGL mRNA was expressed in CB1+/Gad1+ MSDB neurons. Robust CB1- and DAGL-dependent DSI was observed in the MHb, indicating that 2-AG mediates short-term synaptic depression of GABA input. Further, as DSI was observed with optogenetic stimulation of MSDB input, it is apparent that 2-AG acts at GABAergic MSDB axon terminals in the ventral MHb. Consistent with the study identifying the MSDB as the only known GABAergic input to the MHb[22], DSI was abolished in MSDB-CB1-KO mice, suggesting that the MSDB is the only CB1-expressing GABA input to ventral MHb neurons. As $GABA_A$ receptor activation can be excitatory in the MHb due to low expression of KCC2[28], GABA release onto MHb neurons may trigger activity-dependent feedback suppression of GABA release via 2-AG.

CB1 expressed in presynaptic terminals of MHb neurons projecting to the interpeduncular nucleus (IPN) regulates the expression of aversive memories[51]. We investigated the effects of loss- or gain-of function of 2-AG/CB1 signaling in the ventral MHb after MSDB-specific CB1 or MAGL KO on anxiety- and depressive-like behavior. MSDB-specific CB1 knockout led to elevated anxiety-like behavior in multiple behavior tests, including the open field, marble burying, and NSF tests. The increased avoidance behavior in the OFT was similar to that in global CB1 knockout mice[52]. Systemic treatment with the CB1 antagonist rimonabant similarly increased latency to feed in the NSF test[53, 54]. These results suggest that CB1 expressed in MSDB neurons may be a critical locus mediating avoidance and novelty-induced hypophagia. The minimal impact of MSDB-CB1 knockout on light dark box and EPM behavior suggests that these behaviors are regulated by 2-AG/CB1 signaling in other neural pathways. Interestingly, MSDB-MAGL-KO mice had minimal effects on anxiety-like behavior across all behavior tests. This may be because these behavior tests do not evoke high levels of anxiety that are amenable to anxiolytic manipulations. Consistent with this, systemic MAGL inhibition had anxiolytic and antidepressant-like behavioral effects in mice that were exposed to chronic unpredictable stress (CUS), but not those without CUS exposure[4, 5]. Furthermore, MAGL is expressed in both neurons and astrocytes, and both limit 2-AG signaling at synapses[55, 56]. MAGL in local MHb astrocytes may therefore limit excessive 2-AG levels from strongly suppressing MSDB GABA input to the MHb. It also remains possible that 2-AG and anandamide collectively act to regulate anxiety-like behavior, as MSDB-CB1-KO would also abolish the effects of anandamide. Although JZL184 but not URB597 prolonged DSI in the MHb, tonic regulation of synaptic input by anandamide may act in parallel with 2-AG to suppress MSDB GABA release onto ventral MHb neurons. Together, these results suggest that eCB signaling in the MSDB-MHb pathway may have anxiolytic and antidepressant-like effects.

Immobility in the FST reflects behavioral despair and a depressive phenotype[47]. Although neither group differed significantly from control mice, we observed significantly greater immobility time in MSDB-CB1-KO mice than in MSDB-MAGL-KO mice. Additionally, we found that MSDB-MAGL-KO mice had increased sucrose preference. As novelty-suppressed feeding and sucrose preference are sensitive to chronic antidepressant treatment[43, 45], these results collectively suggest that bidirectional modulation of 2-AG/CB1 signaling in the MHb after MSDB-specific KO has opposing effects on depressive-like behavior.

MSDB-CB1-KO abolished DSI in the ventral MHb, indicating a complete loss of 2-AG-mediated depression of GABA release in the ventral MHb. Although this KO is not specific for the MSDB-MHb pathway, the anxiety- and depression-related behaviors may be due to effects in this pathway. RNAscope FISH demonstrated that >90% of MSDB CB1-expressing neurons co-express Gad1, indicating that this CB1 knockout predominantly affects MSDB GABA neurons. Additionally, CB1 expression in MSDB glutamate neurons is comparatively low, and MSDB cholinergic neurons are primarily known to regulate hippocampal theta oscillations[57] and not anxiety or depressive-like behavior. Additional projection targets of MSDB GABA neurons are inhibitory interneurons in the hippocampus and entorhinal cortex[58, 59], but hippocampal interneurons do not display DSI[60], suggesting that MSDB GABA neurons in this pathway may not express CB1 or MAGL. These data are consistent with the hypothesis that the behavioral consequences of MSDB-specific CB1 or MAGL knockout are perhaps mediated by the MSDB-MHb pathway. Although approaches for pathway-specific gene knockout have recently been established in mice[11], the small size of the MHb makes it highly technically challenging to bilaterally inject viral vectors selectively in the MHb in enough mice for behavioral studies. Though we provide evidence for a role of the MSDB-MHb pathway in mediating the behavioral effects of MSDB-specific CB1 or MAGL knockout, the contributions of other MSDB output projections cannot be excluded.

There are limited studies on the role of the MHb in anxiety or depressive disorders in humans. The human MHb is enriched for genes that are negatively correlated with hedonic well-being[61]. Post-mortem histological analysis revealed reduced volume and neuronal cell numbers in the MHb in patients with depression[18]. Post-mortem analysis of the habenula in suicide victims diagnosed with major depressive disorder observed significantly reduced mRNA expression of components of cholinergic signaling, including the choline transporter (SLC5A7) and the β3 subunit of the nicotinic acetylcholine receptor (CHRNB3)[62]. Functional MRI in individuals with generalized anxiety disorder revealed increased functional connectivity of the habenula with regions associated with threat anticipation and avoidance behavior, such as the prefrontal cortex and orbitofrontal cortex[63]. As a link between the basal forebrain and serotonergic midbrain nuclei by way of the IPN, the MSDB-MHb pathway is positioned to transduce cortical information processing and evaluative decision-making to the control of monoamine release. Further, as CB1 antagonists increase brain serotonin levels[64], the MSDB-MHb pathway may be a link between cannabinoid signaling and serotonin release. Interestingly, the IPN and serotonergic dorsal and median raphe project back to the MS[65, 66], thereby forming a polysynaptic loop of synaptically connected structures. Thus, the MSDB-MHb pathway could be an important neural correlate of anxiety and/or depressive disorders amenable to targeted modulation.

In summary, we provide evidence that CB1/eCB signaling suppresses synaptic GABA input to cholinergic neurons of the ventral MHb specifically via actions at CB1-expressing MSDB axon terminals, and that eCBs released from MHb neurons may have anxiolytic and antidepressant-like behavioral effects via suppression of this GABAergic MSDB-MHb pathway (Supplementary Fig. 11). This may be a potential mechanism whereby endocannabinoids can exert anxiolytic and antidepressant-like effects.

Methods and Materials

Animals

Animal maintenance and use were in accordance with protocols approved by the Institutional Animal Care and Use Committee of The Medical College of Wisconsin. Mice were given *ad libitum* access to food and water, unless stated otherwise, and housed four to five per cage in a temperature (23 ± 1°C) and humidity-controlled room (40–60%) with a 14 hr light, 10 hr dark cycle. All experiments were performed on adult (8–16 weeks old at the beginning of the experiments) male or female mice. C57BL/6J (Jax stock#: 000664), Gad2-Cre (*Gad2*$^{tm2(cre)Zjh}$/J, Jax stock#: 010802), ChAT-Cre (*Chat*$^{tm2(cre)Lowl}$/J, Jax stock#: 006410), and Ai9 reporter mice (B6.Cg-Gt(ROSA)26Sor$^{tm9(CAG\text{-}tdTomato)Hze}$/J; Jax stock#: 007909) were obtained from the Jackson Laboratory (Bar Harbor, Maine). ChAT-Cre mice were originally on a mixed C57BL/6;129 background and were backcrossed to C57BL/6J mice. *Cnr1*$^{loxP/loxP}$ mice (Cnr1$^{tm1.1Zxx}$, MGI: 6119514) were generously provided by Zheng-Xiong Xi at NIDA/NIH and were maintained on a C57BL/6J background[67]. *Magl*$^{loxP/loxP}$ mice were generated as described in our previous study[68] and maintained on a C57BL/6J background. ChAT-tdTomato reporter mice were generated by crossing ChAT-Cre mice with Ai9 mice, which express tdTomato following Cre-mediated recombination[27].

Animal surgery and microinjection of AAVs

Mice were anesthetized with ketamine (90 mg/kg, i.p.) and xylazine (10 mg/kg, i.p.) and placed in a stereotaxic device (Neurostar, Tubingen, Germany). For injections into the MSDB, injections were made at the following coordinates: AP 0.86 mm; ML 0.00 mm; DV 4.78–4.80 mm. AAV1.hSyn.HI.eGFP-Cre.WPRE.SV40 (1.78×10^{12} GC/ml) was obtained from the Penn Vector Core of the University of Pennsylvania (Philadelphia, PA). AAV1-phSyn1(S)-Flex-tdTomato-T2A-SypEGFP-WPRE (1.12×10^{12} GC/ml) was obtained from the Viral Vector Core of Salk Institute. AAV_{DJ}-ChR2(H134R)-GFP (1.40×10^{13} GC/ml) was obtained from Neuroscience Gene Vector and Virus Core of Stanford University. AAVs were injected in a volume of 200 nl. The AAV injections were delivered through a Nanoject III Programmable Nanoliter Injector (Drummond Scientific Company, Broomall, PA). The injection rate was 60 nl/min and the injectors were kept in place for 5 min to ensure adequate diffusion from the injector tip. After the surgery, animals received subcutaneous injections of analgesic (buprenorphine-SR, 1 mg/kg). There was a minimum of 3–4 weeks given between AAV injection and electrophysiological, behavioral, or anatomical experiments to allow for sufficient time for transgene expression or genetic knockout.

Behavior

Animal numbers and sample sizes are calculated based on statistical power analysis (α = 5%, Power = 0.8), with consideration of prior experience and sample sizes generally used in the field. Mice were assigned to groups without randomization. The experimenters were blinded to the treatment groups and genotypes of animals when analyzing behavioral tests that require manual scoring (e.g. forced swim test, marble burying test). Behavioral tests have been described in detail in our recent study[4]. Less stressful behavioral tests were performed before more stressful behavioral tests. Behavioral tests were conducted in the

order listed below with only one behavioral test conducted per day. Mice were handled for 3 days prior to the first behavioral test. A complete timeline for the behavior experiments is provided in Fig. 5a.

Open Field Test (OFT)—Mice were placed individually in one corner of an open field (50 cm length × 45 cm width × 30 cm depth box) and allowed to freely explore the arena during a 10 min test session. Locomotor activity was recorded using an automated video-tracking system (ANY-maze; Stoelting, Wood Dale, IL). Total distance traveled and time spent in the center of the box was calculated. Center time is defined as the amount of time that was spent in the central 25 cm × 22.5 cm area of the open field.

Elevated Plus Maze (EPM)—The elevated plus maze apparatus (Stoelting, Wood Dale, IL) consists of two open arms (35 × 5 cm) across from each other and perpendicular to two closed arms (35 × 5 × 15 cm) that are connected by a center platform (5 × 5 cm). The apparatus is elevated 40 cm above the floor. Mice were placed in the center platform facing a closed arm and allowed to freely explore the maze for 5 min. The location of the mice was tracked with ANY-maze. The time spent in open arms and the number of entries into open arms were quantified.

Light-Dark Box (LDB)—Mice were placed individually in an apparatus (46 cm length × 20 cm width × 20 cm depth) with two compartments. One compartment (30 cm length × 20 cm width × 20 cm depth) is exposed to light and has white walls, whereas the other compartment (16 cm length × 20 cm width × 20 cm depth) is covered and has black walls. An opening (6 cm tall × 5 cm wide) separates the two compartments. Mice were placed in the light side and allowed to freely move throughout a 5 min session. Time spent in the light side and number of entries into the light side were tracked using ANY-maze (Stoelting, Wood Dale, IL).

Marble Burying Test (MBT)—Mice were placed individually in their home cage (30 cm length × 18 cm width × 12 cm depth) filled with bedding 7–8 cm deep. Twenty-four dark blue marbles (1.35 cm diameter) were placed on top of the bedding. Mice were allowed to freely move throughout a 20 min session without a cage lid. The number of marbles buried at the end of the 20 min session were counted. Marbles were considered buried if at least two thirds of an individual marble was covered in bedding.

Sucrose Preference (SP)—Mice were individually housed and trained to drink from two drinking bottles for 48 hr. One bottle contained 1% sucrose (in tap water) and the other contained tap water. During the SPT, mice were deprived of food and water for 8 hr, and the consumption of sucrose solution and water over the next 16 hr was measured. Sucrose preference (%) was calculated as sucrose solution consumed divided by the total amount of solution consumed.

Novelty-Suppressed Feeding (NSF)—The NSF test was carried out similar to our previous study[69]. Mice were food deprived for 24 hr before being placed in a novel environment (a plastic box 50 cm long × 35 cm wide × 30 cm deep) where 2–3 food pellets (regular chow) were placed on a piece of white filter paper (8 cm in diameter) in the

center of the box. A mouse was placed in one corner of the box and the latency to feed was measured. Feeding was defined as biting the food with the use of fore-paws, but not simply sniffing or touching the food. Immediately after the test, the animal was transferred to the home cage, and the latency to feed in the home cage was measured to serve as a control.

Forced Swim Test (FST)—Mice were placed individually into glass cylinders (13 cm diameter, 25 cm tall) filled to a depth of ~18 cm with water (30 ± 1°C). The mice were placed in the cylinders for 6 min. The time spent immobile during the last 4 min was scored. Immobility was defined as the cessation of all movements (e.g., climbing, swimming) except those necessary for the mouse to keep its head above water (i.e., floating).

Slice preparation and electrophysiology

Brain slices containing the medial habenula were prepared as described in our recent study[70]. Briefly, mice were anesthetized by isoflurane inhalation and decapitated. The brain was embedded in low-melting- point agarose, and coronal slices (200 μm thick) containing the medial habenula were cut using a vibrating microtome (Leica VT1200s). Slices were cut in a choline-based solution containing the following (in mM): 110 choline chloride, 2.5 KCl, 1.25 NaH_2PO_4, 0.5 $CaCl_2$, 7 $MgSO_4$, 26 $NaHCO_3$, 25 glucose, 11.6 sodium ascorbate, and 3.1 sodium pyruvate at room temperature. After slice cutting, artificial cerebrospinal fluid (ACSF) was progressively spiked into the choline solution every 5 min for 20 min at room temperature to gradually reintroduce Na^+, similar to a previous method[71]. ACSF contained the following (in mM): 119 NaCl, 3 KCl, 2 $CaCl_2$, 1 MgCl2, 1.25 NaH_2PO_4, 25 $NaHCO_3$, and 10 glucose. The slices were allowed to recover for at least an additional 30 min in ACSF prior to recording. All solutions were saturated with 95% O_2 and 5% CO_2.

Whole-cell and cell-attached patch clamp recordings were made from neurons in the MHb using patch-clamp amplifiers (Multiclamp 700B) under infrared differential interference contrast microscopy, as described in our previous study[69]. Data acquisition and analysis were performed using DigiData 1440A and 1550B digitizers and analysis software pClamp 10 (Molecular Devices). Signals were filtered at 2 kHz and sampled at 10 kHz. Neurons were voltage-clamped at −70 mV unless stated otherwise. $GABA_A$ postsynaptic currents were recorded in the presence of the AMPA receptor antagonist 6-cyano-7-nitroquinoxaline-2,3-dione (CNQX; 20 μM). Electrical stimulation was delivered by a bipolar tungsten stimulation electrode (WPI) placed ≥50 μm from the recorded neuron. Pressure ejection of the $GABA_A$ agonist muscimol (2 μM) was via a puff pipette (1–2 μm tip opening, 5 psi, 1 s). Tetanic stimulation was delivered as 5 pulses of electrical stimulation at 50 Hz. For whole-cell recordings of reversal potential and picrotoxin/CNQX sensitivity of MSDB-ChR2-induced currents in MHb neurons, glass pipettes (4–6 MΩ) were filled with an internal solution containing the following (in mM): 100 Cs-methanesulfonate, 40 CsCl, 10 NaCl, 1 EGTA, 0.1 $CaCl_2$, 2 Mg-ATP, 0.3 Na_2-GTP, pH to 7.2 with CsOH. Depolarization to 0 mV for DSI induced large inward currents in Cs-based internal solutions (not shown), likely via activation of Ca^{2+}-activated Cl^- channels[72], precluding the use of Cs-based solutions for these recordings. DSI and all other whole-cell recordings used an internal solution containing the following (in mM): 90 K-gluconate, 50 KCl, 10 HEPES, 0.2 EGTA, 2 $MgCl_2$, 4 Mg-ATP, 0.3 Na_2GTP, and 10 Na_2-phosphocreatine, pH 7.2 with

KOH. Cell-attached recordings of MHb neurons were carried out similar to a previous study[73]. For cell-attached recordings of action potential firing, glass pipettes were filled with ACSF and 0 or 10 μM of the fluorescent dye Alexa 594 to monitor for "spontaneous" mini-breaks into whole-cell mode, detectable by dye diffusion into the recorded cell. For slice optogenetics experiments, blue laser stimulation (473 nm, 3 ms; Laserglow Technologies, Ontario, Canada) was delivered by an optical fiber (200 μm diameter, 0.37 or 0.39 NA, Thorlabs) placed either directly (~50 μm) above the recorded cell or in contact with the slice, therefore providing localized illumination. Series resistance (10–30 MΩ) was monitored throughout all whole-cell recordings, and data were discarded if the resistance changed by > 20%. All recordings were performed at 31 ± 1°C using an automatic temperature controller (Warner Instruments, Inc.).

RNAscope *in situ* hybridization

Mice were deeply anesthetized with isoflurane and transcardially perfused with 0.1 M sodium phosphate buffered saline (PBS) followed by 4% paraformaldehyde in 4% sucrose-PBS (pH 7.4). After perfusion, the brain was removed and post-fixed in the same fixative for 4 hr at 4°C and was then dehydrated in increasing concentrations of sucrose (20% and 30%) in 0.1 M PBS at 4°C and frozen on dry ice. Coronal MHb or MSDB sections (10 μm) were cut with a Leica cryostat (Leica CM1860) and mounted on Superfrost Plus microscope slides (Fisher Scientific). Probes targeting the mRNA transcripts of DAGLα (target region: base pairs 396–1259 of *Mus musculus* diacylglycerol lipase alpha, NM_198114.2), Tac1 (target region: base pairs 20–1034 of *Mus musculus* tachykinin 1, NM_009311.2), ChAT (target region: base pairs 1090–1952 of *Mus musculus* choline acetyltransferase, NM_009891.2), CB1 (target region: base pairs 530–1458 of *Mus musculus* cannabinoid receptor 1, NM_007726.3), VGluT2 (target region: base pairs 1986–2998 of *Mus musculus* vesicular glutamate transporter 2, NM_080853.3), and GAD1 (target region: base pairs 62–3113 of *Mus musculus* glutamate decarboxylase 1, NM_008077.4), were designed by and purchased from Advanced Cell Diagnostics Inc. (Hayward, CA). The experiment was carried out as per the manufacturer's instructions for the RNAscope Multiplex Fluorescent V2 Assay. Stained slides were counterstained with DAPI and mounted with Vectashield Antifade Mounting Medium (Vector Laboratories) and imaged on a Leica TCS SP8 confocal microscope. A probe targeting *Bacillus subtilis* protein DapB was used as a negative control, whereas probes targeting the ubiquitously-expressed Polr2a, PPIB, and UBC served as positive controls. Tyramide signal amplification (TSA®)-conjugated fluorescein, cyanine 3, and cyanine 5 at 1:1000 dilutions were used (Akoya Biosciences). Identical experimental and confocal imaging settings were used to quantify and compare relative expression levels of CB1 in MSDB neuron populations. Imaris (Bitplane) was used for imaging data quantification. The "spots" tool was used to identify and quantify individual fluorescent puncta, which represent one mRNA molecule and therefore provides a measure of mRNA expression[25]. Cyanine 5 was used for CB1 and DAGLα probes to minimize non-specific autofluorescence. Negative control-stained slides were always imaged at the settings used for target probe imaging and did not result in appreciable signal, particularly for cyanine 5-linked targets.

Immunohistochemistry—Mice were anaesthetized by ketamine (90 mg/kg, i.p.) and xylazine (10 mg/kg, i.p.) and transcardially perfused with 0.1 M sodium phosphate buffered saline (PBS) followed by 4% paraformaldehyde in 4% sucrose-PBS (pH 7.4). After perfusion, the brain was removed and post-fixed in the same fixative for 4 hours at 4°C, and was then dehydrated in increasing concentrations of sucrose (20% and 30%) in 0.1 M PBS at 4°C and frozen on dry ice. Coronal MSDB and MHb sections (20 μm) were cut with a Leica cryostat (Leica CM1860). MHb sections were washed with PBS and then incubated with blocking solution (0.3% Triton X-100 + 5% normal donkey serum in PBS) for 2 hours. MHb sections were incubated with primary antibodies against Gephyrin (mouse, 1:500, #147011; Synaptic systems) or MAP2 (Rabbit, 1:500, #188002; Synaptic systems) at 4°C for 24 hours. MHb sections were then incubated with secondary antibodies: Cy™5 AffiniPure donkey anti-Mouse IgG (1:100, 3715175151, Jackson ImmunoResearch) or Alexa Fluor 647 donkey anti-Rabbit IgG (1:100, #A21245, Thermo Fisher Scientific) for 4 hours at room temperature in the dark. MSDB sections were rehydrated in PBS and permeabilized with 0.1% Triton X-100 in PBS followed by 640/660 Deep-Red Fluorescent Nissl stain (N-21483) incubation for 20 min.

Statistical and data analysis

Sample sizes for electrophysiological experiments are based on our previous studies[55, 56, 69, 70] and those commonly used in the field[73]. Data are presented as the mean ± SEM. The magnitude of DSI was calculated as follows: DSI (%) = 100 × [1 – (mean of 2 IPSCs after depolarization/mean of 5 IPSCs before depolarization)]. The decay time constant (τ) of DSI was measured using a single exponential function of $y = y_0 + k \times \exp(-x/\tau)$. Values of two to four DSI trials were averaged for each neuron. Unpaired Student's *t*-tests were used to analyze differences in DSI magnitude and decay time constants between drug pretreatment conditions and between MSDB knockouts. Action potential firing frequency during tetanic electrical stimulation (50 Hz, 5 pulse) was analyzed between the first and last stimulation pulses. Action potential firing frequency in response to muscimol pressure ejection was analyzed from the 3 sec period beginning from the onset of muscimol pressure ejection (1 s duration). The percent increase in firing frequency to tetanic stimulation was calculated as the AP firing frequency during the tetanic stimulation period relative to a 2 sec baseline period. The percent increase in firing frequency to muscimol pressure ejection was calculated as the AP firing frequency during the 3 sec after muscimol application relative to a 5 sec baseline period. Paired Student's *t*-tests were used to analyze before-and-after drug treatments in single neurons. Behavioral results were analyzed using one-way ANOVA followed by Tukey's *post hoc* tests for multiple comparisons when the Shapiro-Wilk normality test and equal variance test indicated normally distributed data with equal variances ($p > 0.05$). With non-normally distributed data (Shapiro-Wilk test $p < 0.05$), or data with un-equal variances (equal variance test $p < 0.05$), one-way ANOVA on Ranks (Kruskal-Wallis test) followed by Dunn's *post hoc* tests for multiple comparisons were used. DAGLα mRNA expression density in Tac1- or ChAT-expressing MHb neurons was quantified for each individually-identified MHb and statistically analyzed via unpaired Student's *t*-test.

Data Availability

All data necessary for evaluation of the paper's conclusions are present in the main text and/or Supplementary information.

Supplementary Material

Refer to Web version on PubMed Central for supplementary material.

Acknowledgements

This work was supported by National Institutes of Health Grants MH115536 (to C.R.V.), MH121454 (to Q.-S.L. and C.J.H.), DA047269 (to Q.-S.L.), and DA035217 (to Q.-S.L.). It was also partially funded through the Research and Education Initiative Fund, a component of the Advancing a Healthier Wisconsin endowment at the Medical College of Wisconsin. CRV is a member of the Medical Scientist Training Program at MCW, which is partially supported by a training grant from NIGMS T32-GM080202.

References

1. Walsh Z, Gonzalez R, Crosby K, M ST, Carroll C, Bonn-Miller MO. Medical cannabis and mental health: A guided systematic review. Clinical psychology review 2017; 51: 15–29. [PubMed: 27816801]
2. Sexton M, Cuttler C, Finnell JS, Mischley LK. A Cross-Sectional Survey of Medical Cannabis Users: Patterns of Use and Perceived Efficacy. Cannabis Cannabinoid Res 2016; 1(1): 131–138. [PubMed: 28861489]
3. Blankman JL, Simon GM, Cravatt BF. A comprehensive profile of brain enzymes that hydrolyze the endocannabinoid 2-arachidonoylglycerol. Chemistry & biology 2007; 14(12): 1347–1356. [PubMed: 18096503]
4. Zhong P, Wang W, Pan B, Liu X, Zhang Z, Long JZ et al. Monoacylglycerol lipase inhibition blocks chronic stress-induced depressive-like behaviors via activation of mTOR signaling. Neuropsychopharmacology : official publication of the American College of Neuropsychopharmacology 2014; 39(7): 1763–1776. [PubMed: 24476943]
5. Zhang Z, Wang W, Zhong P, Liu SJ, Long JZ, Zhao L et al. Blockade of 2-arachidonoylglycerol hydrolysis produces antidepressant-like effects and enhances adult hippocampal neurogenesis and synaptic plasticity. Hippocampus 2015; 25(1): 16–26. [PubMed: 25131612]
6. Bedse G, Bluett RJ, Patrick TA, Romness NK, Gaulden AD, Kingsley PJ et al. Therapeutic endocannabinoid augmentation for mood and anxiety disorders: comparative profiling of FAAH, MAGL and dual inhibitors. Translational psychiatry 2018; 8(1): 92. [PubMed: 29695817]
7. Bedse G, Hartley ND, Neale E, Gaulden AD, Patrick TA, Kingsley PJ et al. Functional Redundancy Between Canonical Endocannabinoid Signaling Systems in the Modulation of Anxiety. Biological psychiatry 2017; 82(7): 488–499. [PubMed: 28438413]
8. Jenniches I, Ternes S, Albayram O, Otte DM, Bach K, Bindila L et al. Anxiety, Stress, and Fear Response in Mice With Reduced Endocannabinoid Levels. Biological psychiatry 2016; 79(10): 858–868. [PubMed: 25981172]
9. Shonesy BC, Bluett RJ, Ramikie TS, Baldi R, Hermanson DJ, Kingsley PJ et al. Genetic disruption of 2-arachidonoylglycerol synthesis reveals a key role for endocannabinoid signaling in anxiety modulation. Cell reports 2014; 9(5): 1644–1653. [PubMed: 25466252]
10. Cravatt BF, Giang DK, Mayfield SP, Boger DL, Lerner RA, Gilula NB. Molecular characterization of an enzyme that degrades neuromodulatory fatty-acid amides. Nature 1996; 384(6604): 83–87. [PubMed: 8900284]
11. Marcus DJ, Bedse G, Gaulden AD, Ryan JD, Kondev V, Winters ND et al. Endocannabinoid Signaling Collapse Mediates Stress-Induced Amygdalo-Cortical Strengthening. Neuron 2020; 105(6): 1062–1076 e1066. [PubMed: 31948734]

12. Shen CJ, Zheng D, Li KX, Yang JM, Pan HQ, Yu XD et al. Cannabinoid CB1 receptors in the amygdalar cholecystokinin glutamatergic afferents to nucleus accumbens modulate depressive-like behavior. Nat Med 2019; 25(2): 337–349. [PubMed: 30643290]
13. Hsu YW, Wang SD, Wang S, Morton G, Zariwala HA, de la Iglesia HO et al. Role of the dorsal medial habenula in the regulation of voluntary activity, motor function, hedonic state, and primary reinforcement. The Journal of neuroscience : the official journal of the Society for Neuroscience 2014; 34(34): 11366–11384. [PubMed: 25143617]
14. Xu C, Sun Y, Cai X, You T, Zhao H, Li Y et al. Medial Habenula-Interpeduncular Nucleus Circuit Contributes to Anhedonia-Like Behavior in a Rat Model of Depression. Front Behav Neurosci 2018; 12: 238. [PubMed: 30356828]
15. Molas S, DeGroot SR, Zhao-Shea R, Tapper AR. Anxiety and Nicotine Dependence: Emerging Role of the Habenulo-Interpeduncular Axis. Trends in pharmacological sciences 2017; 38(2): 169–180. [PubMed: 27890353]
16. Yamaguchi T, Danjo T, Pastan I, Hikida T, Nakanishi S. Distinct roles of segregated transmission of the septo-habenular pathway in anxiety and fear. Neuron 2013; 78(3): 537–544. [PubMed: 23602500]
17. Zhao-Shea R, DeGroot SR, Liu L, Vallaster M, Pang X, Su Q et al. Increased CRF signalling in a ventral tegmental area-interpeduncular nucleus-medial habenula circuit induces anxiety during nicotine withdrawal. Nat Commun 2015; 6: 6770. [PubMed: 25898242]
18. Ranft K, Dobrowolny H, Krell D, Bielau H, Bogerts B, Bernstein HG. Evidence for structural abnormalities of the human habenular complex in affective disorders but not in schizophrenia. Psychol Med 2010; 40(4): 557–567. [PubMed: 19671211]
19. Suarez J, Ortiz O, Puente N, Bermudez-Silva FJ, Blanco E, Fernandez-Llebrez P et al. Distribution of diacylglycerol lipase alpha, an endocannabinoid synthesizing enzyme, in the rat forebrain. Neuroscience 2011; 192: 112–131. [PubMed: 21756982]
20. Kano M, Ohno-Shosaku T, Hashimotodani Y, Uchigashima M, Watanabe M. Endocannabinoid-mediated control of synaptic transmission. Physiological reviews 2009; 89(1): 309–380. [PubMed: 19126760]
21. Castillo PE, Younts TJ, Chavez AE, Hashimotodani Y. Endocannabinoid signaling and synaptic function. Neuron 2012; 76(1): 70–81. [PubMed: 23040807]
22. Qin C, Luo M. Neurochemical phenotypes of the afferent and efferent projections of the mouse medial habenula. Neuroscience 2009; 161(3): 827–837. [PubMed: 19362132]
23. Gray JA, McNaughton N. The neuropsychology of anxiety : an enquiry into the functions of the septo-hippocampal system. 2nd edn. Oxford University Press: Oxford; New York, 2000, xvi, 424 p.pp.
24. Pratt JA. The neuroanatomical basis of anxiety. Pharmacology & therapeutics 1992; 55(2): 149–181. [PubMed: 1363249]
25. Wang F, Flanagan J, Su N, Wang LC, Bui S, Nielson A et al. RNAscope: a novel in situ RNA analysis platform for formalin-fixed, paraffin-embedded tissues. J Mol Diagn 2012; 14(1): 22–29. [PubMed: 22166544]
26. Okamoto Y, Morishita J, Tsuboi K, Tonai T, Ueda N. Molecular characterization of a phospholipase D generating anandamide and its congeners. The Journal of biological chemistry 2004; 279(7): 5298–5305. [PubMed: 14634025]
27. Madisen L, Zwingman TA, Sunkin SM, Oh SW, Zariwala HA, Gu H et al. A robust and high-throughput Cre reporting and characterization system for the whole mouse brain. Nature neuroscience 2010; 13(1): 133–140. [PubMed: 20023653]
28. Kim U, Chung LY. Dual GABAergic synaptic response of fast excitation and slow inhibition in the medial habenula of rat epithalamus. J Neurophysiol 2007; 98(3): 1323–1332. [PubMed: 17615126]
29. Choi K, Lee Y, Lee C, Hong S, Lee S, Kang SJ et al. Optogenetic activation of septal GABAergic afferents entrains neuronal firing in the medial habenula. Sci Rep 2016; 6: 34800. [PubMed: 27703268]

30. Gorlich A, Antolin-Fontes B, Ables JL, Frahm S, Slimak MA, Dougherty JD et al. Reexposure to nicotine during withdrawal increases the pacemaking activity of cholinergic habenular neurons. Proc Natl Acad Sci U S A 2013; 110(42): 17077–17082. [PubMed: 24082085]

31. Reiner A, Veenman CL, Medina L, Jiao Y, Del Mar N, Honig MG. Pathway tracing using biotinylated dextran amines. J Neurosci Meth 2000; 103(1): 23–37.

32. McMahon HT, Bolshakov VY, Janz R, Hammer RE, Siegelbaum SA, Südhof TC. Synaptophysin, a major synaptic vesicle protein, is not essential for neurotransmitter release. Proceedings of the National Academy of Sciences of the United States of America 1996; 93(10): 4760–4764. [PubMed: 8643476]

33. Pizzarelli R, Griguoli M, Zacchi P, Petrini EM, Barberis A, Cattaneo A et al. Tuning GABAergic Inhibition: Gephyrin Molecular Organization and Functions. Neuroscience 2020; 439: 125–136. [PubMed: 31356900]

34. Dehmelt L, Halpain S. The MAP2/Tau family of microtubule-associated proteins. Genome Biology 2004; 6(1): 204. [PubMed: 15642108]

35. Sotty F, Danik M, Manseau F, Laplante F, Quirion R, Williams S. Distinct electrophysiological properties of glutamatergic, cholinergic and GABAergic rat septohippocampal neurons: novel implications for hippocampal rhythmicity. J Physiol 2003; 551(Pt 3): 927–943. [PubMed: 12865506]

36. Gulyas AI, Cravatt BF, Bracey MH, Dinh TP, Piomelli D, Boscia F et al. Segregation of two endocannabinoid-hydrolyzing enzymes into pre- and postsynaptic compartments in the rat hippocampus, cerebellum and amygdala. Eur J Neurosci 2004; 20(2): 441–458. [PubMed: 15233753]

37. Yu T, Guo M, Garza J, Rendon S, Sun XL, Zhang W et al. Cognitive and neural correlates of depression-like behaviour in socially defeated mice: an animal model of depression with cognitive dysfunction. The international journal of neuropsychopharmacology 2011; 14(3): 303–317. [PubMed: 20735879]

38. Patel S, Hillard CJ. Role of endocannabinoid signaling in anxiety and depression. Current topics in behavioral neurosciences 2009; 1: 347–371. [PubMed: 21104391]

39. Bourin M, Hascoet M. The mouse light/dark box test. European journal of pharmacology 2003; 463(1–3): 55–65. [PubMed: 12600702]

40. Prut L, Belzung C. The open field as a paradigm to measure the effects of drugs on anxiety-like behaviors: a review. European journal of pharmacology 2003; 463(1–3): 3–33. [PubMed: 12600700]

41. Hogg S A review of the validity and variability of the elevated plus-maze as an animal model of anxiety. Pharmacol Biochem Behav 1996; 54(1): 21–30. [PubMed: 8728535]

42. de Brouwer G, Fick A, Harvey BH, Wolmarans W. A critical inquiry into marble-burying as a preclinical screening paradigm of relevance for anxiety and obsessive-compulsive disorder: Mapping the way forward. Cogn Affect Behav Neurosci 2019; 19(1): 1–39. [PubMed: 30361863]

43. Bodnoff SR, Suranyi-Cadotte B, Quirion R, Meaney MJ. A comparison of the effects of diazepam versus several typical and atypical anti-depressant drugs in an animal model of anxiety. Psychopharmacology 1989; 97(2): 277–279. [PubMed: 2567028]

44. Rex A, Voigt JP, Voits M, Fink H. Pharmacological evaluation of a modified open-field test sensitive to anxiolytic drugs. Pharmacol Biochem Behav 1998; 59(3): 677–683. [PubMed: 9512071]

45. Liu MY, Yin CY, Zhu LJ, Zhu XH, Xu C, Luo CX et al. Sucrose preference test for measurement of stress-induced anhedonia in mice. Nature protocols 2018; 13(7): 1686–1698. [PubMed: 29988104]

46. Rizvi SJ, Pizzagalli DA, Sproule BA, Kennedy SH. Assessing anhedonia in depression: Potentials and pitfalls. Neuroscience and biobehavioral reviews 2016; 65: 21–35. [PubMed: 26959336]

47. Castagne V, Moser P, Roux S, Porsolt RD. Rodent models of depression: forced swim and tail suspension behavioral despair tests in rats and mice. Current protocols in neuroscience 2011; Chapter 8: Unit 8 10A.

48. Zhang GW, Shen L, Zhong W, Xiong Y, Zhang LI, Tao HW. Transforming Sensory Cues into Aversive Emotion via Septal-Habenular Pathway. Neuron 2018; 99(5): 1016–1028 e1015. [PubMed: 30122379]
49. Koppensteiner P, Galvin C, Ninan I. Development- and experience-dependent plasticity in the dorsomedial habenula. Molecular and cellular neurosciences 2016; 77: 105–112. [PubMed: 27793697]
50. Maccarrone M Metabolism of the Endocannabinoid Anandamide: Open Questions after 25 Years. Frontiers in molecular neuroscience 2017; 10(166): 166. [PubMed: 28611591]
51. Soria-Gomez E, Busquets-Garcia A, Hu F, Mehidi A, Cannich A, Roux L et al. Habenular CB1 Receptors Control the Expression of Aversive Memories. Neuron 2015; 88(2): 306–313. [PubMed: 26412490]
52. Jacob W, Yassouridis A, Marsicano G, Monory K, Lutz B, Wotjak CT. Endocannabinoids render exploratory behaviour largely independent of the test aversiveness: role of glutamatergic transmission. Genes Brain Behav 2009; 8(7): 685–698. [PubMed: 19563475]
53. Bluett RJ, Baldi R, Haymer A, Gaulden AD, Hartley ND, Parrish WP et al. Endocannabinoid signalling modulates susceptibility to traumatic stress exposure. Nat Commun 2017; 8: 14782. [PubMed: 28348378]
54. Gamble-George JC, Conger JR, Hartley ND, Gupta P, Sumislawski JJ, Patel S. Dissociable effects of CB1 receptor blockade on anxiety-like and consummatory behaviors in the novelty-induced hypophagia test in mice. Psychopharmacology 2013; 228(3): 401–409. [PubMed: 23483200]
55. Chen Y, Liu X, Vickstrom CR, Liu MJ, Zhao L, Viader A et al. Neuronal and Astrocytic Monoacylglycerol Lipase Limit the Spread of Endocannabinoid Signaling in the Cerebellum. eNeuro 2016; 3:e0048–16.
56. Liu X, Chen Y, Vickstrom CR, Li Y, Viader A, Cravatt BF et al. Coordinated regulation of endocannabinoid-mediated retrograde synaptic suppression in the cerebellum by neuronal and astrocytic monoacylglycerol lipase. Sci Rep 2016; 6: 35829. [PubMed: 27775008]
57. Vandecasteele M, Varga V, Berenyi A, Papp E, Bartho P, Venance L et al. Optogenetic activation of septal cholinergic neurons suppresses sharp wave ripples and enhances theta oscillations in the hippocampus. Proc Natl Acad Sci U S A 2014; 111(37): 13535–13540. [PubMed: 25197052]
58. Justus D, Dalugge D, Bothe S, Fuhrmann F, Hannes C, Kaneko H et al. Glutamatergic synaptic integration of locomotion speed via septoentorhinal projections. Nature neuroscience 2017; 20(1): 16–19. [PubMed: 27893726]
59. Freund TF, Antal M. GABA-containing neurons in the septum control inhibitory interneurons in the hippocampus. Nature 1988; 336(6195): 170–173. [PubMed: 3185735]
60. Hoffman AF, Riegel AC, Lupica CR. Functional localization of cannabinoid receptors and endogenous cannabinoid production in distinct neuron populations of the hippocampus. Eur J Neurosci 2003; 18(3): 524–534. [PubMed: 12911748]
61. Le Foll B, French L. Transcriptomic Characterization of the Human Habenula Highlights Drug Metabolism and the Neuroimmune System. Front Neurosci 2018; 12: 742. [PubMed: 30429765]
62. Han S, Yang SH, Kim JY, Mo S, Yang E, Song KM et al. Down-regulation of cholinergic signaling in the habenula induces anhedonia-like behavior. Sci Rep 2017; 7(1): 900. [PubMed: 28420875]
63. Ma Z, Zhong Y, Hines CS, Wu Y, Li Y, Pang M et al. Identifying generalized anxiety disorder using resting state habenular circuitry. Brain imaging and behavior 2019. 10.1007/s11682-019-00055-1.
64. Darmani NA, Janoyan JJ, Kumar N, Crim JL. Behaviorally active doses of the CB1 receptor antagonist SR 141716A increase brain serotonin and dopamine levels and turnover. Pharmacol Biochem Behav 2003; 75(4): 777–787. [PubMed: 12957219]
65. Kaifosh P, Lovett-Barron M, Turi GF, Reardon TR, Losonczy A. Septo-hippocampal GABAergic signaling across multiple modalities in awake mice. Nature neuroscience 2013; 16(9): 1182–1184. [PubMed: 23912949]
66. Acsady L, Arabadzisz D, Katona I, Freund TF. Topographic distribution of dorsal and median raphe neurons with hippocampal, septal and dual projection. Acta Biol Hung 1996; 47(1–4): 9–19. [PubMed: 9124016]

67. Han X, He Y, Bi GH, Zhang HY, Song R, Liu QR et al. CB1 Receptor Activation on VgluT2-Expressing Glutamatergic Neurons Underlies Delta(9)-Tetrahydrocannabinol (Delta(9)-THC)-Induced Aversive Effects in Mice. Sci Rep 2017; 7(1): 12315. [PubMed: 28951549]

68. Viader A, Blankman JL, Zhong P, Liu X, Schlosburg JE, Joslyn CM et al. Metabolic Interplay between Astrocytes and Neurons Regulates Endocannabinoid Action. Cell reports 2015; 12(5): 798–808. [PubMed: 26212325]

69. Zhong P, Vickstrom CR, Liu X, Hu Y, Yu L, Yu HG et al. HCN2 channels in the ventral tegmental area regulate behavioral responses to chronic stress. eLife 2018; 7: e32420. [PubMed: 29256865]

70. Vickstrom CR, Liu X, Zhang Y, Mu L, Kelly TJ, Yan X et al. T-Type Calcium Channels Contribute to Burst Firing in a Subpopulation of Medial Habenula Neurons. eNeuro 2020; 7(4).

71. Ting JT, Lee BR, Chong P, Soler-Llavina G, Cobbs C, Koch C et al. Preparation of Acute Brain Slices Using an Optimized N-Methyl-D-glucamine Protective Recovery Method. J Vis Exp 2018; 132: e53825.

72. Cho CH, Lee S, Kim A, Yarishkin O, Ryoo K, Lee YS et al. TMEM16A expression in cholinergic neurons of the medial habenula mediates anxiety-related behaviors. EMBO Rep 2020; 21(2): e48097. [PubMed: 31782602]

73. Ge F, Mu P, Guo R, Cai L, Liu Z, Dong Y et al. Chronic sleep fragmentation enhances habenula cholinergic neural activity. Mol Psychiatry 2019.

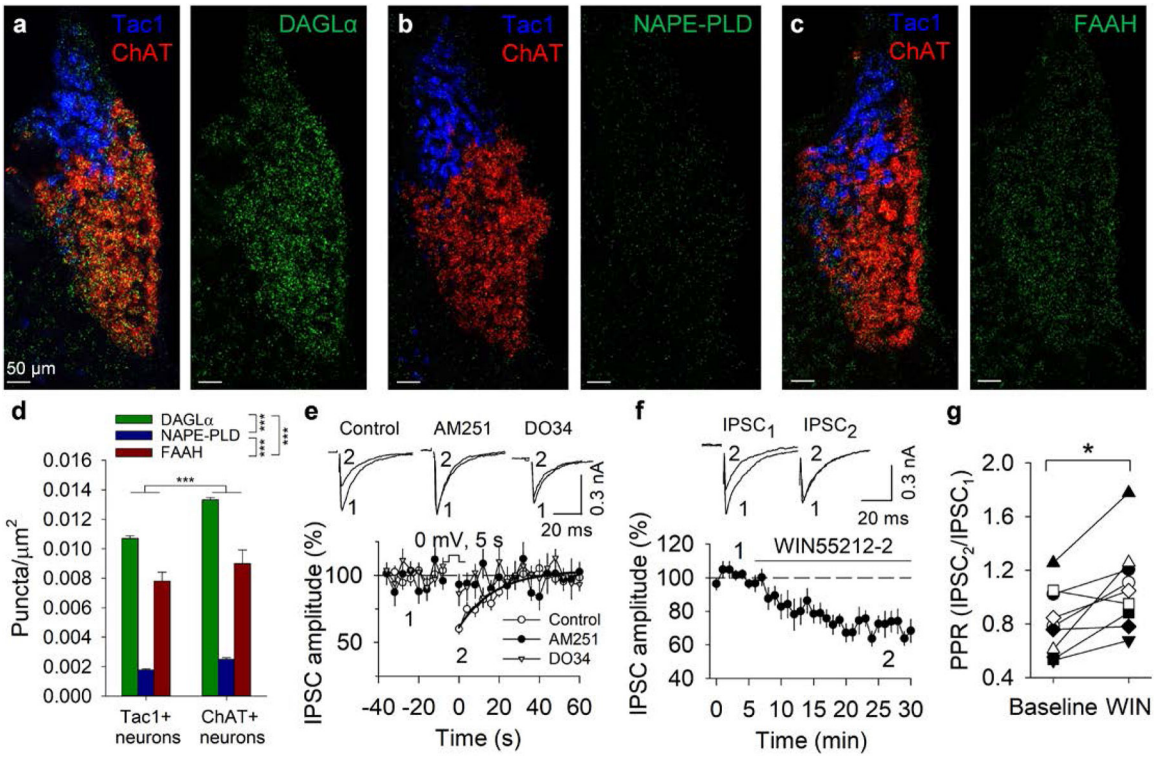

Fig. 1. Expression and function of the endocannabinoid system in the MHb.

a-c. DAGLα, NAPE-PLD, and FAAH mRNA are expressed in the MHb in both Tac1- and ChAT-expressing neurons of the dorsal and ventral MHb. **d.** mRNA puncta density of eCB system components. ChAT+ neurons had a significantly higher mRNA puncta density than Tac1+ neurons (two-way ANOVA significant main effect: $F_{1,42} = 14.803$, $p < 0.001$). DAGLα puncta density was significantly higher than NAPE-PLD ($p < 0.001$) and FAAH puncta density ($p < 0.001$). FAAH puncta density was significantly higher than NAPE-PLD puncta density ($p < 0.001$). **e.** Depolarization (from −70 to 0 mV, 5 s) induced DSI (n = 15 neurons/N = 5 mice), which was blocked by pretreatment with AM251 ($p < 0.001$, n = 9 neurons/N = 2 mice, vs. Control) or DO34 ($p = 0.017$, n = 7 neurons/N = 3 mice, vs. Control). The solid line is a single exponential fitting of the decay of DSI. **f,g.** Perfusion of WIN55212–2 suppressed IPSC amplitude and increased the PPR (50 ms inter-pulse interval; $t_8 = 3.3$, $p = 0.011$, n = 9 neurons/N = 5 mice; paired t-test).

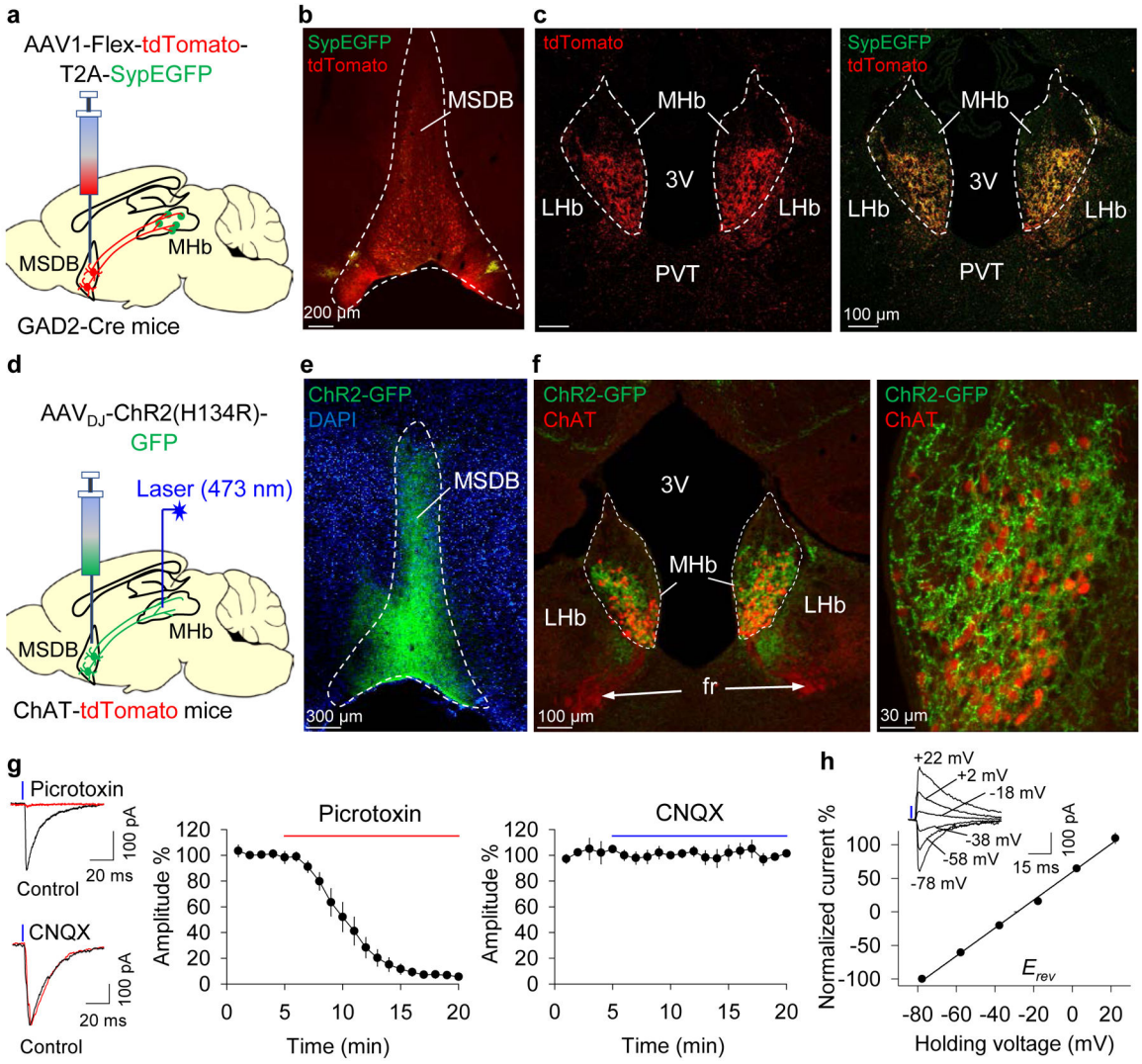

Fig. 2. The MSDB sends an exclusively GABAergic projection to cholinergic neurons in the ventral MHb.

a. Anterograde tracing strategy: cell bodies and axons express tdTomato and putative synaptic puncta express SypEGFP. **b,c.** tdTomato and SypEGFP expression in the MSDB (**b**) and MHb (**c**) after injection of AAV1-Flex-tdTomato-T2A-SypEGFP in the MSDB (n = 3 mice). **d.** Optogenetic circuit mapping strategy: ChR2(H134R)-GFP was expressed in the MSDB and whole-cell recordings of tdTomato+ MHb neurons were made in ChAT-tdTomato reporter mice. **e.** Expression of ChR2-GFP in the MSDB. **f.** ChR2-GFP+ axon terminals were observed in the ventral MHb, where they clustered around tdTomato+ neurons. **g.** Blue (473 nm) light activation of ChR2 on MSDB afferents evoked IPSCs in ventral MHb neurons which were blocked by picrotoxin (n = 9 neurons/N = 3 mice) but were unaffected by CNQX (n = 9 neurons/N = 3 mice). **h.** I-V curve of light-evoked IPSCs shows an average reversal potential (E_{rev}) of −27.8 mV (n = 15 neurons/N = 4 mice). *Inset*: representative light-evoked IPSCs at different junction potential-corrected holding potentials (rounded to nearest integer). Abbreviations: 3V = third ventricle; fr = fasciculus retroflexus; LHb = lateral habenula; MHb = medial habenula; PVT = paraventricular thalamus.

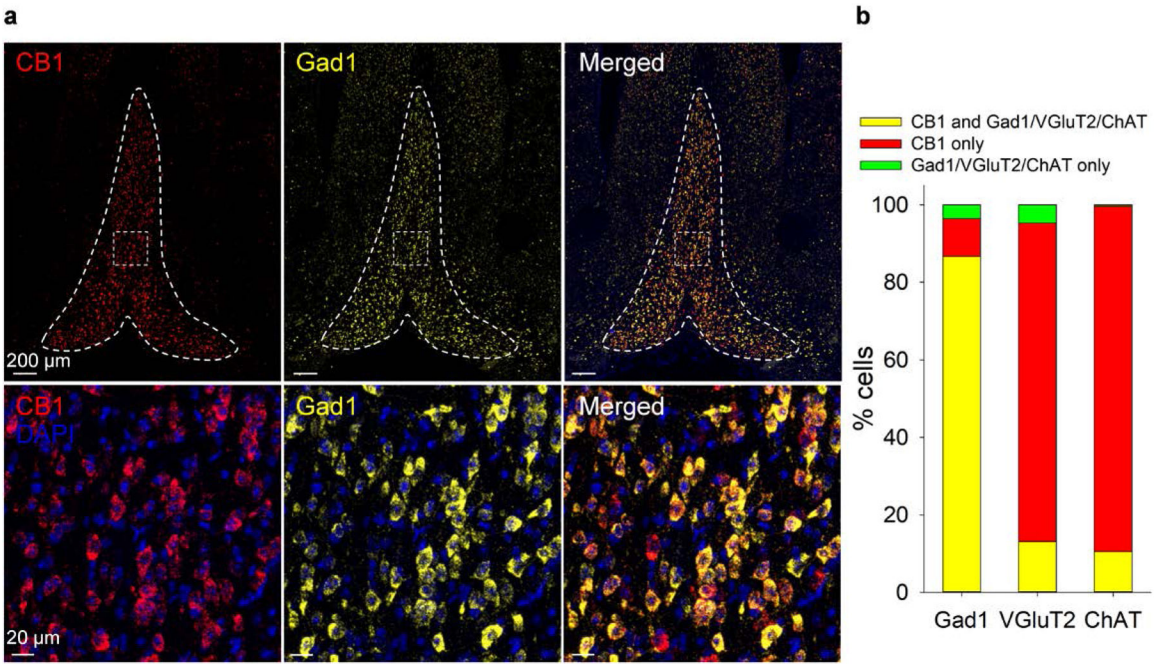

Fig. 3. CB1 receptor mRNA is predominantly expressed in GABA neurons in the MSDB.

a. *Top*: CB1 and Gad1 mRNA are highly expressed in the MSDB. *Bottom*: There is a high degree of CB1 and Gad1 co-expression in the MSDB. **b.** Percentage of cells in the MSDB co-expressing CB1 and/or Gad1, VGluT2, or ChAT, as determined by RNAscope *in situ* hybridization.

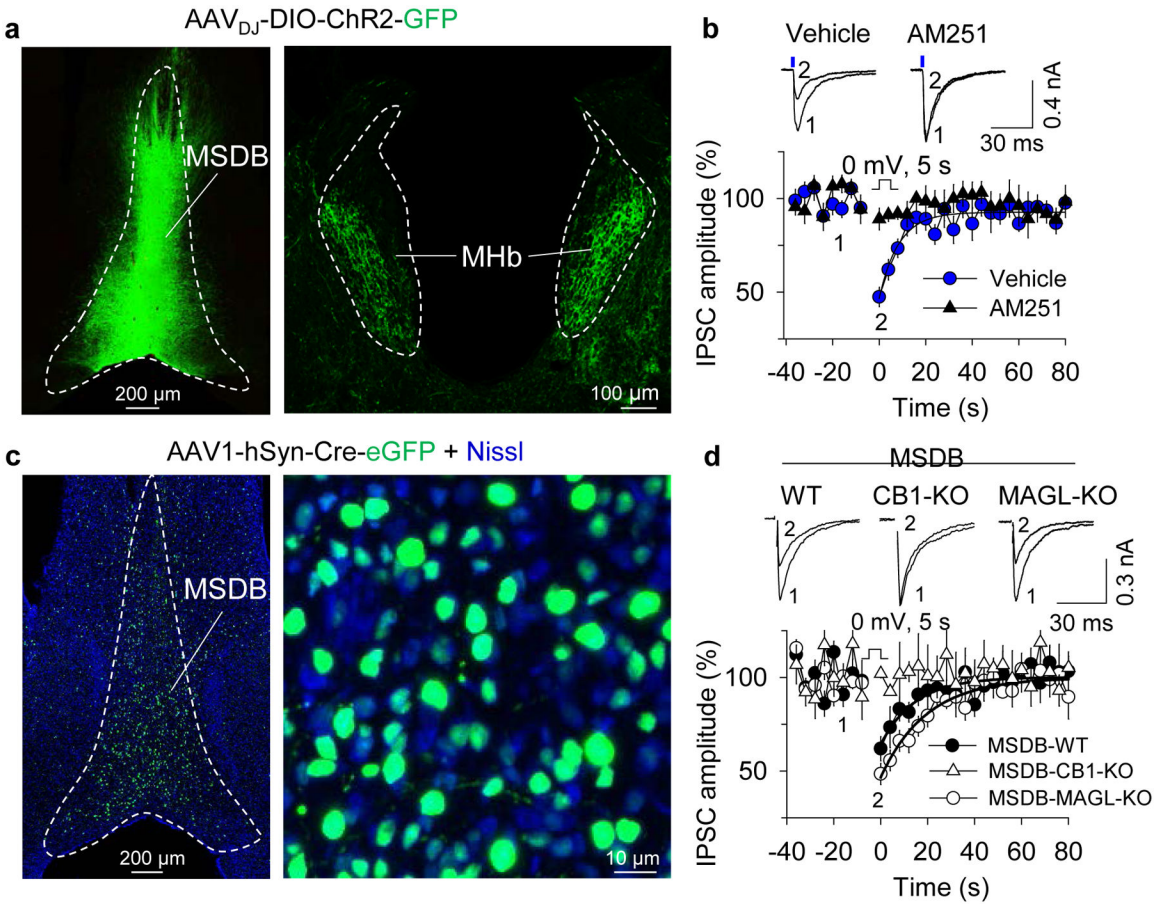

Fig. 4. 2-AG from ventral MHb neurons suppresses MSDB GABA input and is limited by MAGL.

a. AAV$_{DJ}$-DIO-ChR2(H134R)-GFP was injected into the MSDB and ChR2-expressing axon terminals were observed bilaterally in the MHb. **b.** DSI was induced in MHb neurons when IPSCs were evoked by blue laser stimulation of ChR2-expressing MSDB axon terminals. DSI was blocked by AM251 pretreatment (t_{18} = 6.09, p < 0.001, vehicle: n = 12 neurons/N = 4 mice, AM251: n = 8 neurons/N = 3 mice). **c.** AAV1-hSyn-Cre-eGFP was injected into the MSDB to induce schematic for MSDB-specific knockout of CB1 or MAGL. **d.** DSI was abolished in MSDB-CB1-KO mice (MSDB-WT vs. MSDB-CB1-KO, p = 0.023, MSDB-WT: n = 13 neurons/N = 3 mice, MSDB-CB1-KO: n = 8 neurons/N = 3 mice). DSI was prolonged in MSDB-MAGL-KO mice, indicated by an increased time constant of the decay of DSI (MSDB-WT vs. MSDB-MAGL-KO, t_{19} = −2.22, p = 0.039, MSDB-WT: n = 10 neurons/N = 3 mice, MSDB-MAGL-KO: n = 11 neurons/N = 2 mice). The solid lines are single exponential fits of the decay of DSI.

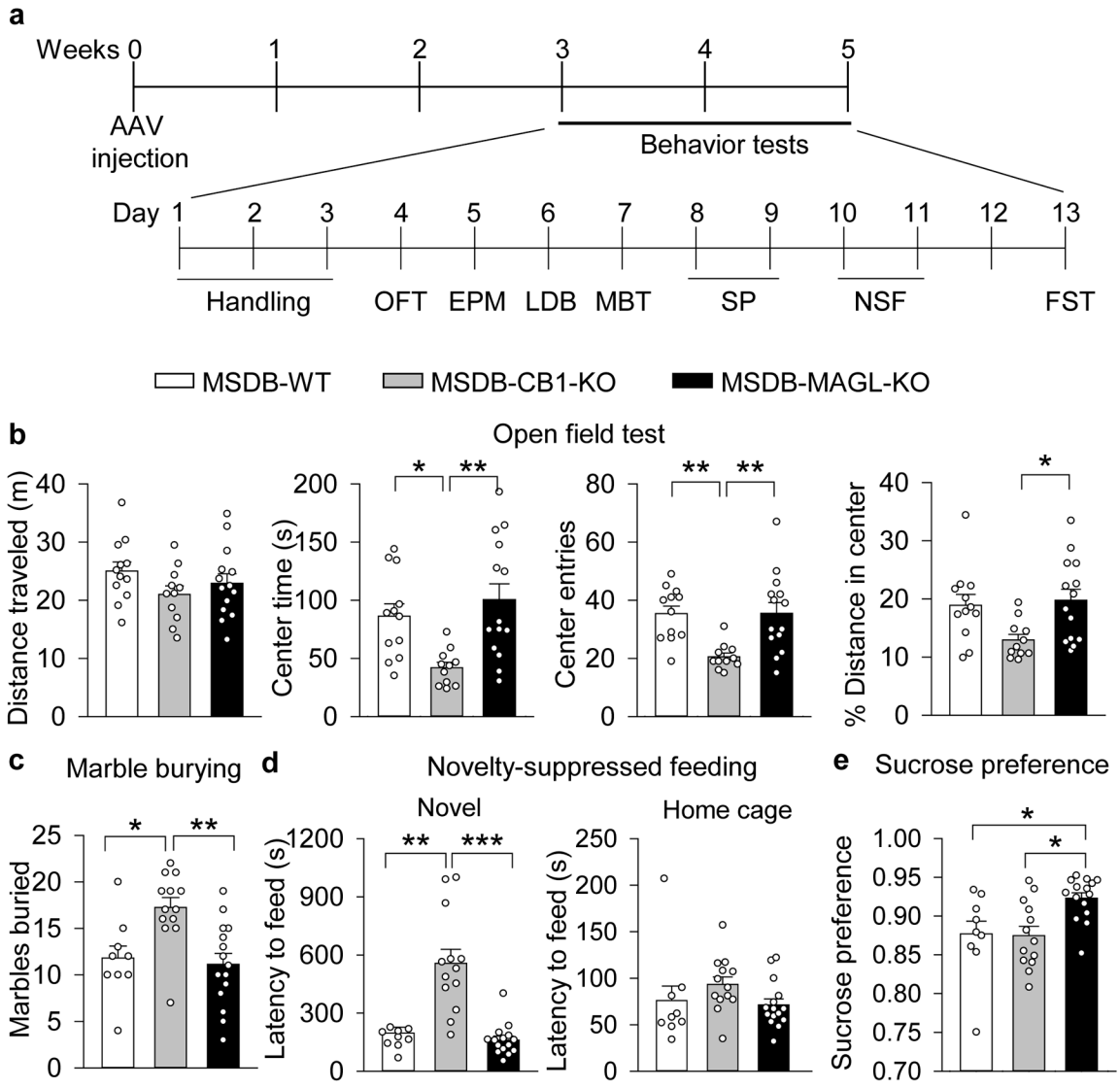

Fig. 5. MSDB-specific CB1 or MAGL knockout has opposing effects on anxiety- and depressive-like behavior.

a. Timeline of AAV injection and behavior tests. **b.** Open field distance traveled was not significantly altered by MSDB knockout ($F_{2,34}$ = 1.524, p = 0.232). Center time in the open field was significantly decreased in MSDB-CB1-KO mice relative to MSDB-WT and MSDB-MAGL-KO mice ($F_{2,34}$ = 7.169, p = 0.003; MSDB-CB1-KO vs. MSDB-WT, p = 0.028; MSDB-CB1-KO vs. MSDB-MAGL-KO, p = 0.002). The number of center entries was significantly reduced in MSDB-CB1-KO mice relative to MSDB-WT and MSDB-MAGL-KO mice ($F_{2,34}$ = 8.207, p = 0.001; MSDB-CB1-KO vs. MSDB-WT, p = 0.004; MSDB-CB1-KO vs. MSDB-MAGL-KO, p = 0.003). The percent distance traveled in the center was significantly reduced in MSDB-CB1-KO mice relative to MSDB-MAGL-KO mice, but was not significantly altered in MSDB-CB1-KO mice relative to MSDB-WT mice ($F_{2,34}$ = 4.571, p = 0.017; MSDB-CB1-KO vs. MSDB-WT, p = 0.056; MSDB-CB1-KO vs. MSDB-MAGL-KO, p = 0.020). MSDB-WT: n = 12; MSDB-CB1-KO: n = 11; MSDB-MAGL-KO: n = 14. **c.** Marble burying behavior was increased in MSDB-CB1-KO

mice ($F_{2,34}$ = 8.076, p = 0.001; MSDB-CB1-KO vs. MSDB-WT mice, p = 0.015; MSDB-CB1-KO vs. MSDB-MAGL-KO mice, p = 0.002). **d.** Novelty-suppressed feeding changes induced by MSDB-specific CB1 or MAGL KO (H = 22.461, p < 0.001; MSDB-CB1-KO vs. MSDB-WT, p = 0.0035; MSDB-CB1-KO vs. MSDB-MAGL-KO, p < 0.001). Home cage feeding behavior was not significantly altered between groups (H = 6.149, p = 0.046; MSDB-WT vs. MSDB-CB1-KO, p = 0.0803; MSDB-WT vs. MSDB-MAGL-KO, p > 0.9999; MSDB-CB1-KO vs. MSDB-MAGL-KO, p = 0.1295). **e.** Sucrose preference increased in MSDB-MAGL-KO mice ($F_{2,34}$ = 6.060, p = 0.006; MSDB-MAGL-KO vs. MSDB-WT mice, p = 0.026; MSDB-MAGL-KO vs. MSDB-CB1-KO mice, p = 0.011). (**c-e**) MSDB-WT: n = 9; MSDB-CB1-KO: n = 13; MSDB-MAGL-KO: n = 15.